







Article

Antibacterial Activity from *Momordica charantia* L. Leaves and Flavones Enriched Phase

Abraão de Jesus B. Muribeca ^{1,†}, Paulo Wender P. Gomes ^{2,3,†}, Steven Souza Paes ¹, Ana Paula Alves da Costa ⁴, Paulo Weslem Portal Gomes ⁵, Jéssica de Souza Viana ¹, José Diogo E. Reis ¹, Sônia das Graças Santa R. Pamplona ¹, Consuelo Silva ^{1,6}, Anelize Bauermeister ⁷, Lourivaldo da Silva Santos ¹ and Milton Nascimento da Silva ^{1,*}

- ¹ Institute of Exact and Natural Sciences, Federal University of Pará, Augusto Corrêa, 01, Guamá, Belém 66075-110, PA, Brazil
- ² Collaborative Mass Spectrometry Innovation Center, University of California San Diego, La Jolla, San Diego, CA 92093, USA
- ³ Skaggs School of Pharmacy and Pharmaceutical Sciences, University of California, La Jolla, San Diego, CA 92093, USA
- ⁴ Department of Natural Science, Campus XIX, State University of Pará, Rodovia PA 154, Km 28, Cajú, Salvaterra 66860-000, PA, Brazil
- ⁵ Institute of Biology, University of Campinas, Monteiro Lobato, 255, Barão Geraldo, Campinas 13083-862, SP, Brazil
- ⁶ Pharmaceutical Science Post-Graduation Program, Faculty of Pharmacy, Federal University of Pará, Belém 66075-110, PA, Brazil
- ⁷ Institute of Biomedical Sciences, University of São Paulo, São Paulo 05508-900, SP, Brazil
- * Correspondence: yumilton@yahoo.com.br; Tel.: +55-91-3201-7365
- † These authors contributed equally to this work.



Citation: Muribeca, A.d.J.B.; Gomes, P.W.P.; Paes, S.S.; da Costa, A.P.A.; Gomes, P.W.P.; Viana, J.d.S.; Reis, J.D.E.; Pamplona, S.d.G.S.R.; Silva, C.; Bauermeister, A.; et al. Antibacterial Activity from *Momordica charantia* L. Leaves and Flavones Enriched Phase. *Pharmaceutics* **2022**, *14*, 1796. <https://doi.org/10.3390/pharmaceutics14091796>

Academic Editor: Yasumasa Ikeda

Received: 9 July 2022

Accepted: 4 August 2022

Published: 26 August 2022

Publisher's Note: MDPI stays neutral with regard to jurisdictional claims in published maps and institutional affiliations.



Copyright: © 2022 by the authors. Licensee MDPI, Basel, Switzerland. This article is an open access article distributed under the terms and conditions of the Creative Commons Attribution (CC BY) license (<https://creativecommons.org/licenses/by/4.0/>).

Abstract: *Momordica charantia* L. (Cucurbitaceae) is a plant known in Brazil as “melão de São Caetano”, which has been related to many therapeutic applications in folk medicine. Herein, we describe antibacterial activities and related metabolites for an extract and fractions obtained from the leaves of that species. An ethanolic extract and its three fractions were used to perform in vitro antibacterial assays. In addition, liquid chromatography coupled to mass spectrometry and the molecular networking approach were used for the metabolite annotation process. Overall, 25 compounds were annotated in the ethanolic extract from *M. charantia* leaves, including flavones, terpenes, organic acids, and inositol pyrophosphate derivatives. The ethanolic extract exhibited low activity against *Proteus mirabilis* (MIC 312.5 $\mu\text{g}\cdot\text{mL}^{-1}$) and *Klebsiella pneumoniae* (MIC 625 $\mu\text{g}\cdot\text{mL}^{-1}$). The ethyl acetate phase showed interesting antibacterial activity (MIC 156.2 $\mu\text{g}\cdot\text{mL}^{-1}$) against *Klebsiella pneumoniae*, and it was well justified by the high content of glycosylated flavones. Therefore, based on the ethyl acetate phase antibacterial result, we suggest that *M. charantia* leaves could be considered as an alternative antibacterial source against *K. pneumoniae* and can serve as a pillar for future studies as well as pharmacological application against the bacteria.

Keywords: glycosylated flavones; molecular networking; dereplication; antibacterial activity

1. Introduction

Clinical infections caused by resistant bacteria have become a major public health concern worldwide, and approximately 700,000 deaths per year are caused by this type of bacteria [1]. It is estimated that by 2050, there will be more than 10 million deaths/year credited to ‘superbugs’, with the expectation of the highest rate being reported in developing countries [2]. The demand for new antimicrobial agents has been growing at the same time as the discovery and advancement of multi-resistant bacteria. Therefore, researchers have been focusing a great effort on the search for new therapeutic alternatives against multidrug-resistant bacteria [3]. In this sense, plant derivatives appear as potential sources of new drugs that act in different ways to deactivate or block the growth of such pathogens [4].

The Cucurbitaceae family includes several species widely distributed throughout the tropical and subtropical regions. There are antimicrobial activities associated with crude extracts and isolated metabolites of species from this family [5]. Among the species, *Momordica charantia* L., popularly known as “melão de São Caetano”, is considered an invasive plant in Brazil and can be found in different places in the country. It is frequently grown in orchards and coffee plantations, or even on fences and debris in abandoned land [6], and is composed of compound classes such as terpenoids, saponins, and flavonoids [5,7]. This species can be highlighted due to its antimicrobial [5], nutraceutical and inflammatory properties [8], as well as healing of gastric ulcers [9], rheumatism [10], and so on. In developing countries, *M. charantia* has been employed in folk medicine for several other pharmacological purposes, such as to treat toothache, diarrhea, furuncle, cancer, hypertension, obesity, bacterial and viral infections, diabetes, pneumonia, and even AIDS [11–16].

Although the chemical characterization of such plants can lead to new pharmaceuticals, it remains challenging due to the presence of several components with different physical–chemical properties, including many in relatively small quantities [17]. Nuclear magnetic resonance (NMR) techniques provide valuable structural information used for structure characterization and therefore, provide unequivocal identification. Liquid chromatography coupled to mass spectrometry (LC-MS) plays a crucial role as it is compatible with chromatographic techniques that allow the separation of compounds in the sample, leading to a deeper investigation of the whole chemical content due to the high sensitivity of MS that can detect metabolites of picomole to femtomole levels in some cases [18]. Furthermore, MS allows the detection of metabolites as ions in the form of mass to charge ratio (m/z) [19], and also allows the fragmentation of the ions at the gas phase by collision-induced dissociation (CID), providing MS/MS spectra that contain valuable information to contribute to annotation of the chemical structure [20]. It is worth mentioning that the acquisition of scan spectra by mass spectrometry is fast, and a single chromatographic run can provide thousands of MS spectra. Therefore, methods that allow a fast and easy analysis of such data are welcome in this field.

In this context, molecular networking, a tool from the Global Natural Products Social Molecular Networking (GNPS) [21] infrastructure, allows the visualization of MS/MS data by organizing it by spectral similarity. This is a very effective strategy, especially because establishing a similarity relationship provides organization into molecular families (usually related chemical structures), and, therefore, finds related metabolites in the dataset even in small amounts. GNPS also contains a spectral library of known compounds, and the molecular networking allows automatic searches in the spectral library, which contributes to speed up the dereplication of known compounds, a phytochemical approach that has been widely used in recent decades, including the modest contribution of these authors [22–26], and which is also unknown by recognition of the analogs into the molecular families.

Based on the antimicrobial potential already reported for *M. charantia*, this study describes the evaluation of in vitro antibacterial activity for the ethanolic extract and fractions from the leaves of *M. charantia*. In addition, liquid chromatography coupled to high-resolution mass spectrometry (LC-HRMS) analyses allowed the chemical characterization of the samples.

2. Materials and Methods

2.1. Botanical Material and Extraction

Leaves of *M. charantia* were collected in the municipality of Soure (0°23'50" S and 49°27'02" W), Marajó Island, PA, Brazil. The botanical material was incorporated (voucher: MFS009218) in the Prof. Dr. Marlene Freitas da Silva (MFS) Herbarium of the State University of Pará. Permission to access the Brazilian genetic patrimony was provided by SISGEN (A695619).

The leaves were washed with water from the Direct-Q5 system (Millipore, Darmstadt, Germany) and decontaminated with sodium hypochlorite solution (NaOCl, 0.1%) acquired from Dinâmica (Jaraguá do Sul, SC, Brazil). The samples were dried in an air circulation oven (Quimis, Brazil) at 45 °C until constant weight. The dry material was crushed in ball mills up to a granulometry of 60 to 100 µm, obtaining 146.54 g. The mass was subjected to extraction with 1 L of ethanol (Tedia, Fairfield, OH, USA) at room temperature for 24 h (2×), and 35.30 g of crude extract was obtained after the solvent evaporation process. Thus, 1 g of ethanolic extract (EE) was mixed with a hydroalcoholic solution, consisting of 60 mL of ultra-pure water, 20 mL of ethanol, and 1 mL of hydrochloric acid (Dinâmica, Indaiatuba, SP, Brazil). The resulting solution was subjected to liquid – liquid partition (LLP) to obtain the hexane (PhHex), ethyl acetate (PhEA), and hydroalcoholic (PhWOH) phases, respectively.

2.2. Liquid Chromatography-High Resolution Mass Spectrometry Analysis

The analyses were performed on a Xevo G2-S QqTOF mass spectrometer (Waters Corp., Milford, MA, USA) equipped with a LockSpray source. The instrument was calibrated with a mass of reference (leucine-enkephalin) utilized for accurate mass measurements. MassLynx 4.1 software was used for system control and data acquisition. The samples were analyzed in a BEH C18 column (Waters Corp.; 50 mm; 2.1 mm; 1.7 µm particle size) using ultra-pure water (solvent A) and acetonitrile (solvent B), both containing 0.1% formic acid. The column temperature was maintained at 40 °C. Linear gradient elution was performed with a flow of 300 µL/min and 5 – 95% of solvent B in 20 min. The injection volume of the samples was 5 µL. The mass spectra data were recorded in a negative ionization mode (ESI) for a mass range from m/z 50 to 1200. The source temperature was set to 120 °C with a cone gas flow of 50 L/h. The desolvation gas flow was set to 600 L/h at a temperature of 150 °C. The capillary was set at 3.0 kV with cone voltage at 40 V. The settings of the data-dependent acquisition (DDA) experiments were: centroid format, number of ions selected 5 (Top5 experiment), the normalized collision energy (NCE) was set to 10, 20, 30, 40 and 50, scan rate of 0.5 sec, charge states of +1 and +2, tolerance window of ±0.2 Da and peak extract window of 2 Da, tolerance of deisotope ± 3 Da, extraction tolerance of deisotope 6 Da.

2.3. Mass Spectrum Data Treatment

The raw files of the EE and PhEA acquired in the Xevo G2-S QTOF mass spectrometer (Waters Corp., Milford, MA, USA) were converted into mzML format using the software MS Convert of the ProteoWizard package [27] and were processed with the software MZmine 2.53 version [28]. The limit for the detection of ions in negative mode at the MS¹ level was set at 1.0×10^3 and MS² at 5.0×10^1 . Chromatograms were constructed using ADAP with a minimum group number of 3 and a minimum group intensity limit of 1.0×10^3 , a min highest intensity of 3.0×10^3 and an m/z tolerance of 10.0 ppm. The local minimum search algorithm was used to deconvolve the chromatogram, with an m/z tolerance of 0.5 for the pairing of MS² and 0.2 min for RT. Isotopes were detected using a peak window with a tolerance of 10.0 ppm, an RT tolerance of 0.5 min, a maximum charge of 1. For peak alignment, the tolerance of m/z 10 ppm was used, scores for m/z of 75 and 25 for RT with a tolerance of 0.2 min. The resulting list was filtered to remove duplicates and lines with no associated MS² spectrum. Then, gap filling was used to fill in the gaps in the peak list. The resultant files were exported using FBMN-GNPS.

2.4. Molecular Networks

The molecular network was built from the mgf and CSV files exported from MZmine. We used metadata to organize metabolite information according to the online workflow (available online: <https://ccms-ucsd.github.io/GNPSDocumentation/>, accessed on 30 January 2022) available on the GNPS website (available online: <http://gnps.ucsd.edu>, accessed on 8 July 2022) [21]. The tolerance of m/z for the precursor ion was adjusted to 0.02 Da and for fragment ion to 0.02 Da. Minimum cosine score above 0.5 and the minimum number of fragment ions were fixed on 4. The spectra on the network were then searched in the GNPS spectral libraries. The database spectra were filtered with a minimum cosine score above 0.6 and a minimum of 4 fragment ions correspondence. The job is available online at the link: <https://gnps.ucsd.edu/ProteoSAFe/status.jsp?task=4890e08934bb4334b8738a346c10e7c4>, accessed on 8 July 2022. The results were visualized and organized using Cytoscape version 3.8.2 (Seattle, WA, USA) [29]. Lastly, the correlation between PhEA and bioactivity score of the metabolites was obtained from NPAnalyst [30].

2.5. In Vitro Antibacterial Assay

Three strains of bacteria were used to evaluate the potential of the extracts: *Staphylococcus aureus* ATCC 25923, and *Klebsiella pneumoniae* ATCC 700603, provided by Instituto Evandro Chagas, Pará State (Brazil) and the bacteria *Proteus mirabilis* LACEN 8/7 (human isolated) provided by the Central Laboratory of Pará State collection. These microorganisms were selected for being common pathogens that can infect humans, animals or plants. The pure cultures were maintained by routine sub-culturing at one-week intervals in BHI broth (Brain Heart Infusion, Kasvi, Spain), incubated at 37 °C, and spiked for 24 h for their metabolic activation. The minimum inhibitory concentration (MIC) and minimum bactericidal concentration (MBC) were conducted using a method approved by the Clinical and Laboratory Standards Institute in 96-well microtitration plates [31].

2.6. Determination of Minimum Inhibitory Concentration (MIC) and Minimum Bactericidal Concentration (MBC)

The antimicrobial susceptibility test was conducted using a method approved by the Clinical and Laboratory Standards Institute [31]. The tests were carried out with a stock solution of 5 mg·mL⁻¹ of the crude extract/phases using the successive dilution method to obtain the concentrations from 2500 to 78.1 µg·mL⁻¹. Ciprofloxacin (Medley, Brazil) and vancomycin (1 mg·mL⁻¹ each) were used as positive controls and BHI (Brain Heart Infusion) culture medium was used as negative control.

A total of 5 mg of extract/phases was dissolved in 100 µL of DMSO (Neon, Brazil) contained in Eppendorf tubes. Then, 900 µL of sterile BHI was added and stirred for better homogenization. In a 96-well microtitration plate (KASVI, Brazil), 100 µL of BHI broth was added to each well. Then, 100 µL of solution containing the samples was added to the first well of each column.

In each well, 5 µL of the bacterial suspension (10⁴ Colony Forming Unit CFU/mL as required by CLSI) was inoculated and adjusted to 0.5 McFarland Standard scale and then the plates were incubated at 37 °C for 24 h. The results were read by adding 10 µL of TTC (2,3,5-triphenyltetrazolic chloride, NEON, Brazil). To prepare the dye, 0.2 g of TTC was added to the penicillin type flask containing 10 mL of sterile distilled water. The final solution showed a translucent color, and when in contact with environments where there are microorganisms presents a red color.

The type of activity presented in each concentration (bacteriostatic or bactericidal) was checked. In the cavities where there was no red color caused by the reaction of TTC with the bacteria, 5 µL of the volume contained in the wells was (re) inoculated in a Petri dish containing BHI agar culture medium and incubated at 37 °C for 24 h. Wells where bacteria grew indicated a bacteriostatic effect at that concentration and wells without bacteria indicated a bactericidal effect.

3. Results and Discussion

3.1. Antibacterial Activity

The EE and the PhEA of *M. charantia* showed antimicrobial activity and, therefore, they were selected to be analyzed by LC-MS/MS. Both positive controls of vancomycin and ciprofloxacin had a MIC of 7.8 $\mu\text{g}\cdot\text{mL}^{-1}$. The EE demonstrated a good bactericidal effect against *Klebsiella pneumoniae* and *Proteus mirabilis*. The PhEA stands out for presenting the best result with a MIC of 156.2 $\mu\text{g}\cdot\text{mL}^{-1}$ for the *K. pneumoniae*, suggesting that this presents bioactive substances, possibly the glycosylated flavones, responsible for such activity (Table 1). We highlighted the bactericidal effect of *Klebsiella Pneumoniae*, and *Proteus Mirabilis*, both Gram-negative strains. The literature [32] reports that the cell wall of Gram-negative bacteria acts as a barrier to a number of substances, including antibiotics. However, recently it was confirmed that quercetin derivatives have strong antibacterial action against Gram-negative bacteria [33], and the ethyl acetate phase (PhEA, see Table 1) described in this study showed high content of quercetin (16) derivatives, i.e., quercetin-*O*-sambubioside (4), quercetin-*O*-glucoside (6), quercetin-*O*-glucosyl-6''-acetate (9), and quercetin-*O*-acetyl-pentoside (13). MIC values < 100 $\mu\text{g}\cdot\text{mL}^{-1}$ are considered significant antimicrobials; moderate inhibitors present MIC in the range of 100 to 625 $\mu\text{g}\cdot\text{mL}^{-1}$; and inhibitors with MIC > 625 $\mu\text{g}\cdot\text{mL}^{-1}$ are considered weak [34]. In this sense, the ethyl acetate phase showed moderate activity (Table 1) against *K. pneumoniae* (MIC of 156.2 $\mu\text{g}\cdot\text{mL}^{-1}$), while the ethanolic extract showed moderate activity against *P. mirabilis* (312.5 $\mu\text{g}\cdot\text{mL}^{-1}$) and weak activity against *K. pneumoniae* and *S. aureus* (625 $\mu\text{g}\cdot\text{mL}^{-1}$). We emphasize that the MIC value against *K. pneumoniae* is in the range moderate-significant, which characterizes PhEA, a source of candidate inhibitors of important hospital bacteria.

Table 1. Bacteria growth behavior in the presence of the extract and phases at different concentrations.

Concentration ($\mu\text{g}\cdot\text{mL}^{-1}$)	EE	PhHex	PhEA	PhWOH	EE	PhHex	PhEA	PhWOH	EE	PhHex	PhEA	PhWOH
	<i>Klebsiella pneumoniae</i>				<i>Proteus mirabilis</i>				<i>Staphylococcus aureus</i>			
2500	=	+	=	+	=	+	−	+	−	+	−	+
1250	=	+	=	+	=	+	+	+	−	+	+	+
625	=	+	=	+	=	+	+	+	−	+	+	+
312.5	+	+	=	+	=	+	+	+	+	+	+	+
156.2	+	+	=	+	+	+	+	+	+	+	+	+
78.1	+	+	+	+	+	+	+	+	+	+	+	+
39.0	+	+	+	+	+	+	+	+	+	+	+	+

Note: NP: natural product; EE: ethanolic extract; PhHex: hexane phase; PhEA: ethyl acetate phase; PhWOH: hydroalcoholic phase; = bactericidal effect; − bacteriostatic effect; + not active.

In previous reports, antimicrobial activity for leaves, fruits and seeds was reported against some clinically important bacteria [20]. The extract of the leaves showed the main results of being a potent inhibitor for *Staphylococcus aureus*, moderate for *Staphylococcus epidermidis* and weak for *Candida albicans*. Studies with extracts of the seed showed interesting activities against *Escherichia coli*, *Salmonella typhi*, and *Staphylococcus aureus*, but less activity against *Pseudomonas aeruginosa* [35].

3.2. Identification of Chemical Constituents

The total ion profiles of the EE and PhEA were recorded from 50 to 1200 Da in 20 min (Figure 1). The molecular formulas, main fragment ions, and putative names are shown in Table 2. A total of 32 major metabolites were detected in the EE. Of these, 25 compounds were annotated in level 2 and 3 of identification according to MSI [36] based on HRMS and MS/MS data and the literature; most of these compounds have well characterized fragmentation (MS/MS) profiles [37].

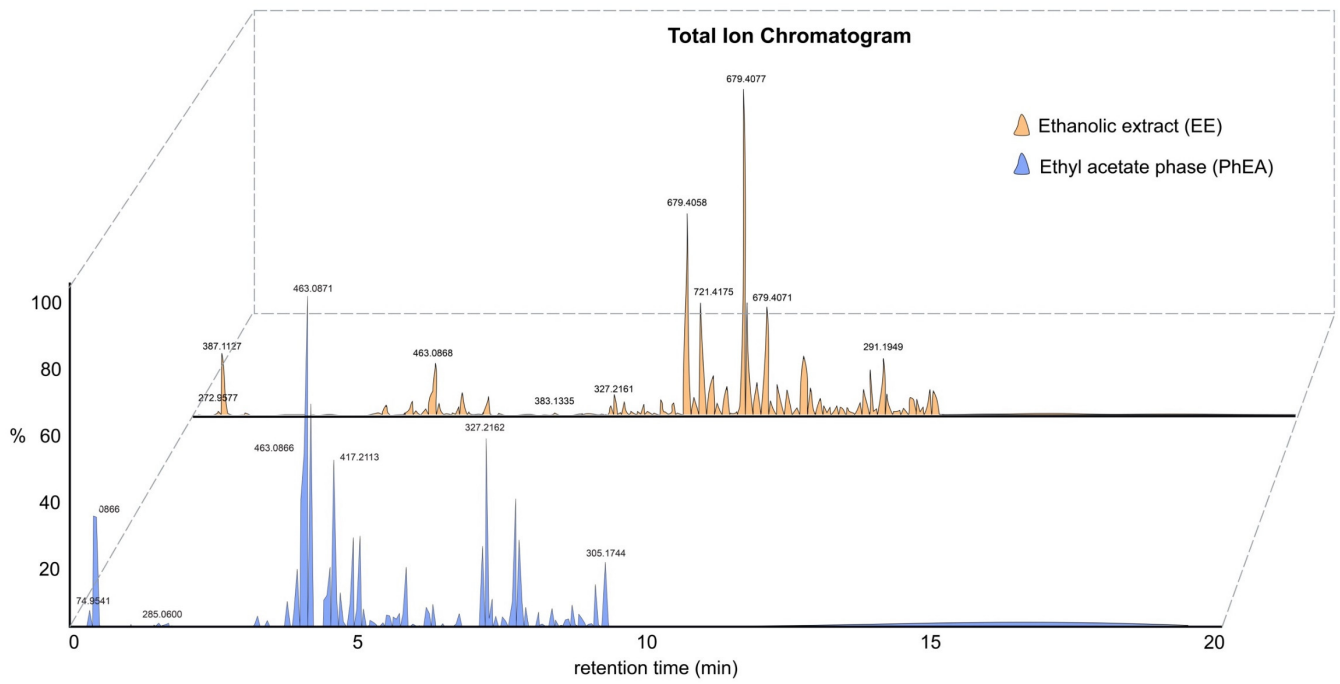


Figure 1. Total ion chromatogram (TIC) in the negative ionization mode of the ethanolic extract (EE), and ethyl acetate phase (PhEA).

Table 2. The identified or tentatively identified compounds of ethanolic extract and ethyl acetate phase from *Momordica charantia* by LC-HRMS.

Peak	Rt (Min)	Molecular Formula	[M – H] [−] (m/z)			Main Product Ions (MS/MS)	Annotated Compound	EE	PhEA
			Calculated	Accurate	Error (ppm)				
1	0.42	C ₁₃ H ₂₄ O ₁₃	387.1139	387.1129	2.6	341, 278, 179	melibiose	x	-
2	1.63	C ₁₂ H ₁₄ O ₈	285.0610	285.0602	2.8	153	dihydrobenzoic acid pentose	x	x
3	3.23	C ₂₀ H ₃₂ O ₁₀	^a 431.1917	^a 431.1910	1.6	385.1856 [M – H] [−] , 223, 205, 163, 119, 113	hydroxy-2,4,4-trimethyl-3-(3-oxobutyl)-2-cyclohexen-1-one glucoside	x	x
4	3.71	C ₂₆ H ₂₈ O ₁₆	595.1299	595.1306	1.2	445, 300, 272, 251, 191, 178	quercetin-O-sambubioside	x	x
5	3.97	C ₂₇ H ₃₀ O ₁₆	609.1456	609.1458	0.3	463, 301	rutin	x	x
6	4.08	C ₂₁ H ₂₀ O ₁₂	463.0877	463.0869	1.7	301, 271, 179	quercetin-O-glucoside	x	x
7	4.14	C ₂₆ H ₂₈ O ₁₅	579.1350	579.1348	0.3	463, 399, 327, 285, 151, 109	kaempferol-O-glucoside-O-pentoside	x	-
8	4.39	C ₂₇ H ₃₀ O ₁₅	593.1506	593.1511	0.8	547, 447, 357, 327, 285	luteolin-O-rutinoside	x	x
9	4.37	C ₂₃ H ₂₂ O ₁₃	505.0982	505.0980	0.4	300, 271, 255, 243, 178, 151	quercetin-O-glucosyl-6''-acetate	x	x
10	4.53	C ₂₁ H ₂₀ O ₁₁	447.0927	447.0926	0.2	327, 284, 255, 227	kaempferol-O-glucoside	x	x
11	4.65	C ₇ H ₆ O ₃	137.0239	137.0228	8.0	93	4-hydroxybenzoic acid	x	-
12	4.67	C ₂₂ H ₂₂ O ₁₂	477.1033	477.1035	0.4	431, 357, 315, 300, 285, 271, 151	isorhamnetin-O-glucoside	x	-
13	4.87	C ₂₃ H ₂₂ O ₁₂	489.1038	489.1033	1.0	285, 255, 227	quercetin-O-acetylpentoside	x	x
14	4.98	C ₂₀ H ₃₄ O ₉	^a 417.2125	^a 417.2113	2.9	371.2052 [M – H] [−] , 209, 161,	icariside B6	x	x
15	5.66	C ₁₈ H ₃₂ O ₇	359.2070	359.2061	2.5	343, 305, 287, 239, 227, 209, 197, 171	unknown	x	-
16	5.77	C ₁₅ H ₁₀ O ₇	301.0348	301.0341	2.3	273, 245, 193, 179, 151, 121	quercetin	x	x
17	7.14	C ₁₈ H ₃₂ O ₅	327.2171	327.2162	2.7	291, 229, 171	trihydroxy octadecadienoic acid isomer	x	x
18	7.24	C ₁₈ H ₃₂ O ₅	327.2171	327.2160	3.3	291, 229, 171	trihydroxy octadecadienoic acid isomer	x	x

Table 2. Cont.

Peak	Rt (Min)	Molecular Formula	[M – H] [−] (m/z)			Main Product Ions (MS/MS)	Annotated Compound	EE	PhEA
			Calculated	Accurate	Error (ppm)				
19	7.64	C ₁₈ H ₃₄ O ₅	329.2328	329.2320	2.4	211, 171	trihydroxy octadecenoic acid	x	x
20	8.38	C ₃₇ H ₆₀ O ₁₁	679.4057	^a 679.4053	0.6	633.3994 [M – H] [−] , 285	momordicoside L isomer	x	-
21	8.58	C ₁₈ H ₂₈ O ₄	307.1909	307.1903	2.0	289, 267, 235, 209, 185	unknown	x	-
22	9.06	C ₃₉ H ₆₀ O ₁₃	^a 735.3956	^a 735.3963	0.9	689.3918 [M – H] [−] , 667, 599, 527, 339	hederagenin base-2H + 1O, O-AcetylHex	x	-
23	9.74	C ₃₉ H ₆₂ O ₁₂	721.4163	721.4156	1.0	675 [M – H] [−] , 633, 513, 275, 193	hederagenin-O-AcetylHex	x	-
24	9.18	C ₁₈ H ₂₆ O ₄	305.1753	305.1746	2.3	287, 249, 207	unknown	x	-
25	9.37	C ₃₇ H ₆₀ O ₁₁	^a 679.4057	^a 679.4060	0.4	633.4015 [M – H] [−] , 575, 549, 471, 343	momordicoside L isomer	x	-
26	9.92	C ₄₆ H ₅₆ O ₆	703.3999	703.4061	0.6	659, 633, 597, 482, 350	unknown	x	-
27	10.0	C ₃₀ H ₆₀ O ₁₆	^a 675.3803	^a 675.3735	10	629.3677 [M – H] [−] , 569, 467, 447, 339, 297	triterpene glycosides derivative	x	x
28	10.4	C ₃₇ H ₆₀ O ₁₁	^a 679.4057	^a 679.4052	0.7	633.4084 [M – H] [−] , 530, 339, 291, 137	momordicoside L isomer	x	-
29	11.51	C ₁₈ H ₂₉ O ₃	293.2117	293.2109	2.7	275, 235, 183, 121	unknown	x	-
30	11.56	C ₂₈ H ₆₂ O ₂₁	733.3705	733.3729	3.3	689, 554, 412, 364, 259, 175	unknown	x	-
31	12.0	C ₃₆ H ₅₄ O ₁₀	645.3639	645.3639	0.0	601, 559, 513, 407, 339, 243, 168, 127	unknown	x	-
32	14.9	C ₃₂ H ₄₄ O ₉	571.2907	571.2882	4.4	525, 481, 391, 325, 315, 255, 241, 153	1-Hexadecanoyl-sn-glycero-3-phospho-(1'-myo-inositol) isomer	x	-

Note: ^a [M + HCOOH – H][−]; EE: ethanolic extract; PhEA: phase ethyl acetate; x: presence; -: absent.

3.3. Molecular Networking (GNPS Annotation)

The molecular networking created with EE and PhEA showed 224 parent ions after removing the blank. Seven compounds (6, 7, 8, 10, 12, 23 and 32) including isomers were annotated based on MS² data available in the GNPS spectral libraries. A family of flavones was reported, and the structure of the compounds is shown in Figure 2.

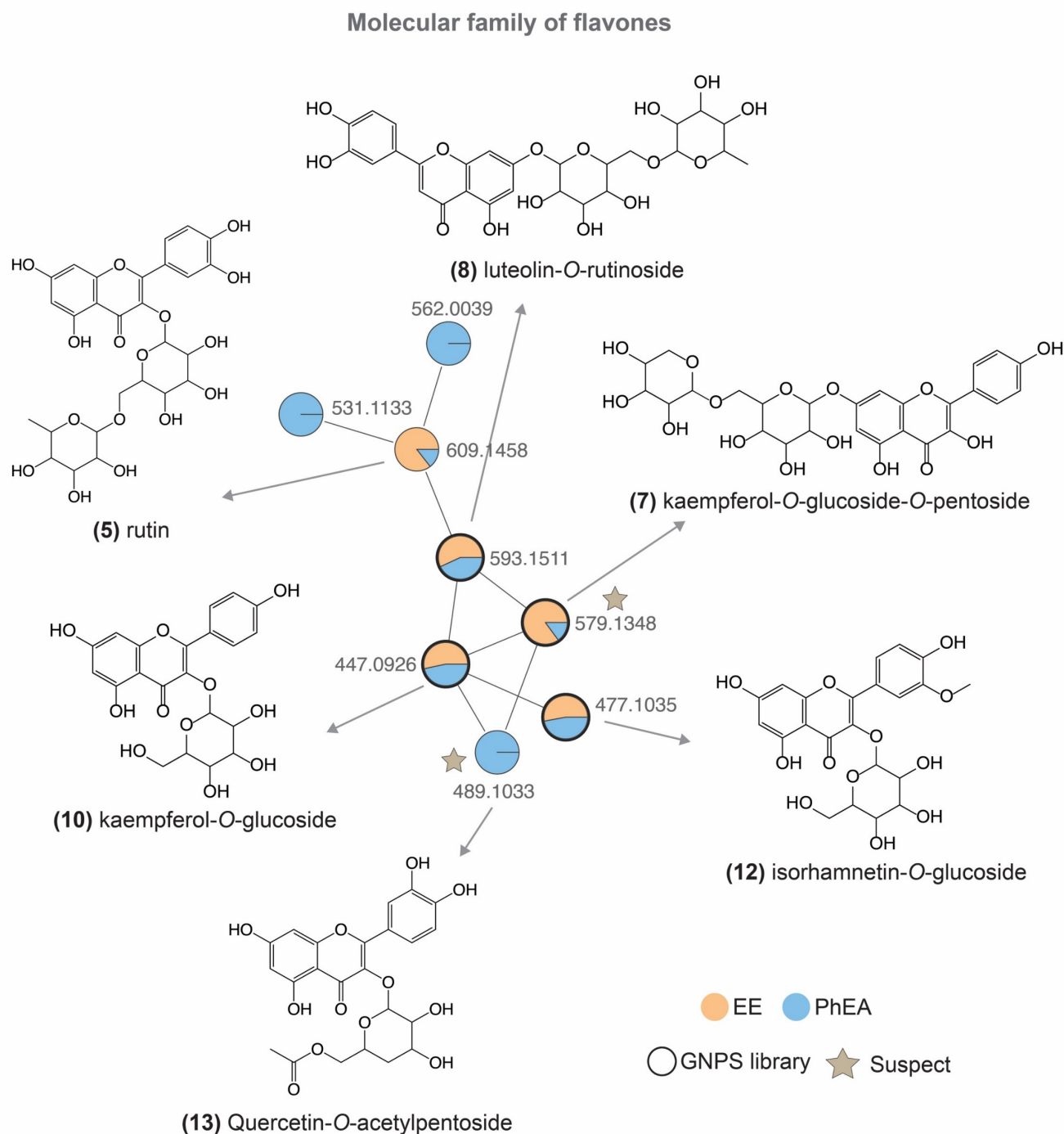


Figure 2. Feature-based molecular networking (GNPS) based on MS/MS data (ESI⁻) from GNPS library [21] and suspect list [38]. The arrows indicate the nodes that have a match in the spectral library and their respective structure. Node text indicates the parent ion, node color reports the extract of the plant (orange: ethanolic extract from leaves; blue: phase ethyl acetate from leaves).

The peak 6 $[M - H]^-$ of m/z 463.0869 with the main fragments m/z 301, 271, and 179 was annotated as quercetin-*O*-glucoside. The loss of the sugar unit $[(M - H) - H_2O]^-$ explains the fragment of m/z 301. However, the position of the hydroxyl groups in ring B, as well as the glycosyl moiety, cannot be confirmed with only MS/MS data. The loss of H_2O following CO $[(M - H) - H_2O - CO]^-$ justifies the m/z 271 [39]; lastly, the loss of $C_7H_6O_2$ on the B ring by retrocyclisation [39] explains the fragment of m/z 179. The peak 7 $[M - H]^-$ of m/z 579.1355 was annotated as kaempferol *O*-glucoside-*O*-pentoside (product ions: m/z 463, 399, 327, 285, 151, 109). The losses of $C_5H_8O_3$ $[(M - H) - C_5H_8O_3]^-$ and $C_7H_{16}O_5$ $[(M - H) - C_5H_8O_3]^-$ confirm the presence of two sugar units in the molecule, however, as discussed before, the positions of the sugar moieties cannot be certainly confirmed. Furthermore, characteristic fission from sugars ($^{0,2} X_1$ mechanism) [40] suggests the m/z 327, the ion of m/z 285, occurs by losses of two sugar units, and the loss of $C_8H_6O_2$ referred to the C ring $[(M - H) - C_8H_6O_2]^-$ explains the ion of m/z 151. The base structure coumarin is identified by loss of $C_9H_4O_4$ to the B ring $[(M - H) - C_9H_4O_4]^-$ characterizing the fragment of m/z 109. The peak 8 $[M - H]^-$ of m/z 593.15 was annotated as luteolin-*O*-rutinoside and this molecule showed main fragments of m/z 547, 447, 357, 327, 285. The loss of C_2H_6O is very common in glycosylated flavones [41], which explains the fragment of m/z 547. In addition, from m/z 593 to 447 loss of $C_6H_{10}O_4$ $[(M - H) - 146]^-$ occurs and from m/z 447 to 285 loss of another sugar unit occurs. Lastly, m/z 285 is confirmed as the aglycone peak. The other fragments are very well discussed in the literature [40]; losses of $C_3H_6O_3$ $[(M - H) - 146 - 90]^-$ and CH_2O $[(M - H) - 146 - 90 - 30]^-$ suggested the ions of m/z 357 and 327, respectively. The peak 10 $[(M - H)]^-$ of m/z 447.0926 was annotated as kaempferol-*O*-glucoside and the fragments of m/z 327, 284, 255, and 227 are very well discussed in the literature [39,42]. In summary, fission of kind $^{0,2} X_1$ occurs in the glycoside to the ion m/z 327, then, the aglycone (m/z 284) is confirmed by radical cleavage $[^3Y_0 - H]^-$ followed by a loss of CH_2O $[^3Y_0 - CH_2O]^-$ and CO $[^3Y_0 - CH_2O - CO]^-$ to the fragments of m/z 255 and 227. The peak 12 $[M - H]^-$ of m/z 477.1035 was annotated as isorhamnetin-*O*-glucoside. The loss of C_2H_6O in the glucoside [41] explains the ion m/z 431 $[(M - H) - 46]^-$ and the $^{0,2} X_1$ mechanism confirms the loss of $C_4H_8O_4$ $[(M - H) - 120]^-$ to the ion of m/z 357. The loss of glucoside occurs as m/z 315 $[(M - H) - C_6H_{10}O_5]^-$ followed by loss of radical CH_3 from m/z 315 $[(M - H) - C_6H_{10}O_5 - CH_3]^\bullet$. Aglycone corresponds to the ion of m/z 285; ion of m/z 271 was formed by a loss of CO_2 $[(M - H) - C_6H_{10}O_5 - CO_2]^-$ and retro-Diels-Alder (RDA) from m/z 151 [43,44].

The peak 32 $[M - H]^-$ of m/z 571.2882 was characterized as 1-hexadecanoyl-sn-glycero-3-phospho-(1'-myo-inositol), an important inositol pyrophosphates derivative present in plants as a signaling metabolite [45–47]. While information about this new class of molecules in plants is still scarce, the enzymes responsible for their synthesis have recently been elucidated [48]. In this sense, 32 is being reported for the first time in the genus. Despite the report of some sulfur-derived compounds in the *M. charantia* sample [49], they were not observed in this work.

A molecular family of glycosylated terpene derivatives (Figure 3) was detected in the EE. The ion of m/z 385.1856 is referent from peak 3, identified as hydroxy-2,4,4-trimethyl-3-(3-oxobutyl)-2-cyclohexen-1-one glucoside, and the pathway of fragmentation has been shown in previous reports [50]. The fragmentation of the ion m/z 385 generated an ion at m/z 223, which refers to a neutral loss of a glycoside $[(M - H) - 162]^-$. A loss of H_2O indicates the ion m/z 205 followed by losses C_2H_2O and C_3H_8 suggesting the ions of m/z 163 $[(M - H) - 42]^-$ and 119 $[(M - H) - 42 - 44]^-$, respectively. Lastly, m/z 113 is explained by ring fission and loss of $C_7H_{10}O$ $[(M - H) - 110]^-$. This compound is included in the monoterpenes class and derivatives already reported in the literature from the Cucurbitaceae family [51].

Molecular family of glycosylated terpenoids and derivatives

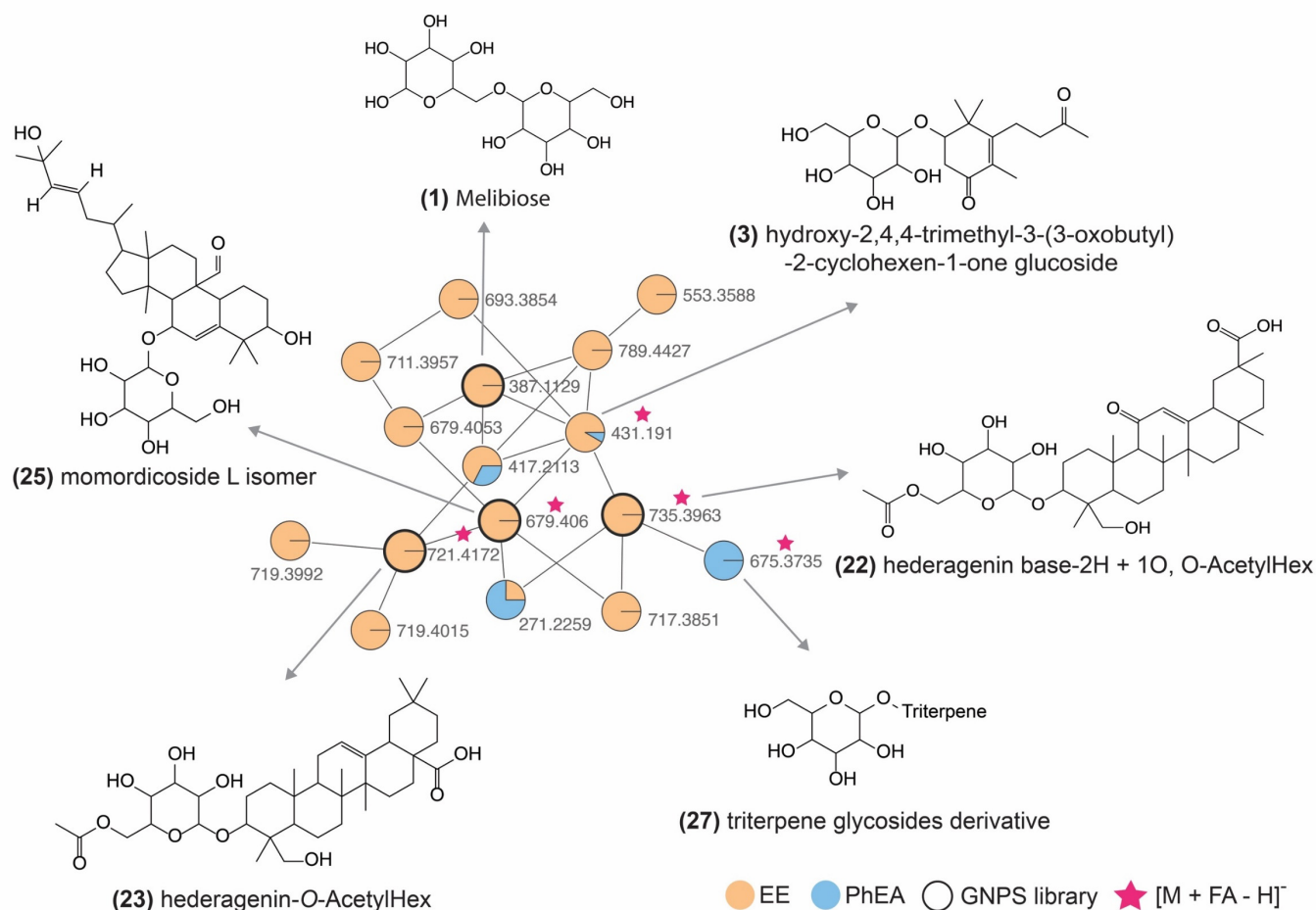


Figure 3. Representation of hydroxy-2,4,4-trimethyl-3-(3-oxobutyl)-2-cyclohexen-1-one glucoside (3) clusters in ethanolic extract using MS/MS in negative ionization mode.

According to Figure 2, the compounds 3, 22, 25, and 27 showed the presence of glycoside. In this sense, following the chemosystematic from the genus, for example, the compound 25 was characterized as momordicoside L isomer, a cucurbitane-type triterpenoid already reported for the species [52]. According to the literature [52], the most intense product ion of m/z 471 corresponds to the aglycone after the loss of glycoside [(M - H) - Glc]⁻, and in addition a loss of C₃H₆O (propan-2-one) in C-5 characterized the ion of m/z 575 [(M - H) - 58]⁻ following loss of C₂H₂ to the fragment of m/z 549. Lastly, the ion of m/z 343 occurs by loss of C₈H₁₆O [(M - H) - Glc - 128]⁻ from the aglycone. Furthermore, this highlights that the cucurbitane is related to the genus [53,54] and confirms the chemosystematic possibility that this study has found an isomer of momordicoside L. The peak 22 showed a match in the GNPS library and it was annotated as hederagenin base-2H + 1O, O-AcetylHex. Peak 27 was suggested as a triterpene glycoside derivative, and we believe it has the same base structure of momordicoside L based on the molecular network. Furthermore, compound 27 has a difference of 4 Da concerning momordicoside L, suggesting two unsaturated bonds. Finally, the compound 23 [M - H]⁻ of m/z 721.4172 was annotated as aederagenin-O-acetyl-hex.

3.4. Bioactivity and Structure

Previous studies reported that flavonoids have antimicrobial activity [55,56]. These stand out even more because of their antibacterial properties, especially against strains of Gram-negative bacteria, which are responsible for serious opportunistic infections and

are resistant to common therapies. In this sense, the study of plants with high flavonoid content should be highlighted [57]. Thus, our study focused on the ethyl acetate phase ($MIC\ 156.2\ \mu\text{g}\cdot\text{mL}^{-1}$) against *K. pneumoniae*, which stands out for its ability to develop enzymatic resistance mechanisms and is considered to be largely responsible for several infectious diseases [58]. The PhEA proved to be rich in flavones, for instance quercetin-*O*-glucoside (6) and luteolin-*O*-rutinoside (8) (Figure 4), which confirms the correlation of the observed antimicrobial activity, as well the EE.

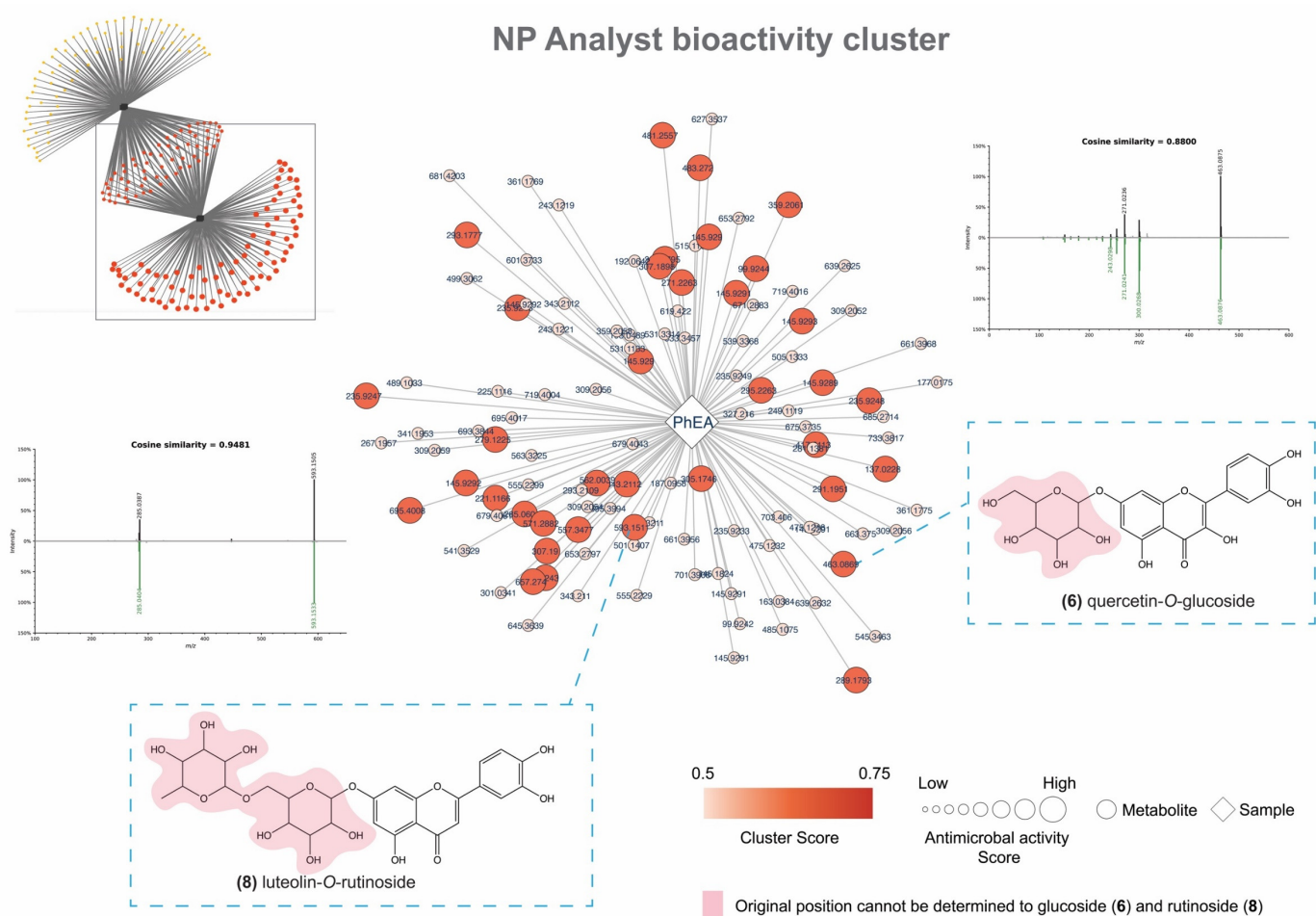


Figure 4. Community network. PhEA illustrated as square white node. Two examples of predicted bioactive flavones (6,8). The color of metabolite nodes is defined by cluster score (0.5–0.75). The size corresponds to the activity score (normalized data).

Our chemical prospecting data summarize chemical constituents that have in common a structural core of flavones, well known for a variety of activities [25]. Furthermore, isolated flavonols such as quercetin and kaempferol already show promising results as antimicrobials [59] as well against *K. pneumoniae* ($MIC > 256\ \mu\text{g}\cdot\text{mL}^{-1}$) [60] and are the base structures of the main protagonists of the PhEA in this study. We emphasize carefully that the nominal results have a much more expressive value than many works given the same biological answer; perhaps the answer may be even more significant if the studies aim at obtaining isolated compounds. However, we emphasize that the rapid annotation provided using the LC-MS/MS technique does not require isolation, but shows an understanding of the active extension of the extract, directing more objective studies to that specific class. In addition, the literature [61] treats enriched phases as the main drivers for more specific studies, not to reach the main compounds responsible for the activity but to exclude those who may be acting as deterrents of the activity. In this sense, we are not being

categorical in pointing only to these substances as active, but we are presenting a more interference-free sample.

4. Conclusions

This study showed the extract and phase ethyl acetate from *M. Charantia* leaves as an antibacterial agent. A total of 32 major compounds were detected, and, of these, 25 were annotated based on mass spectrometry data. Compounds including flavones, terpenes, organic acids, and inositol pyrophosphate derivatives are reported for the first time for the genus *Momordica*. The ethanolic extract exhibited low activity against *Proteus mirabilis* and *Klebsiella pneumoniae*. However, the phase ethyl acetate enriched with flavones showed interesting antibacterial inhibition against *K. pneumoniae*. Hence, we show that the leaves are a renewable antibacterial source and can serve as a pillar for future studies.

Author Contributions: Original design: A.d.J.B.M., P.W.P.G. (Paulo Wender P. Gomes), S.S.P. and A.P.A.d.C. designed this study; A.d.J.B.M. and J.D.E.R. conducted plant extractions and phase separations; S.S.P., A.P.A.d.C. and J.d.S.V. conducted the biological experiments; P.W.P.G. (Paulo Weslem P. Gomes) conducted the botanical identification. Conceptualization, data curation, and formal analysis: A.d.J.B.M., P.W.P.G. (Paulo Wender P. Gomes) and S.S.P. writing—review, visualization and editing: P.W.P.G. (Paulo Wender P. Gomes), S.d.G.S.R.P. C.S., A.B., L.d.S.S. and M.N.d.S. Advisor, funding acquisition and resources: L.d.S.S. and M.N.d.S. Project administration: M.N.d.S. All authors have read and agreed to the published version of the manuscript.

Funding: Coordenação de Aperfeiçoamento de Pessoal de Nível Superior (CAPES), Process: 88882.445 389/2019-01, Modality: Doctoral Scholarship. Pró-reitoria de Pesquisa—Universidade Federal do Pará (UFPA) and Universidade do Estado do Pará (UEPA) for the financial support.

Institutional Review Board Statement: Not applicable.

Informed Consent Statement: Not applicable.

Data Availability Statement: All supporting data used in this study are available from the authors.

Acknowledgments: The authors would like to express their deepest gratitude to Waters Technologies do Brasil LTDA for the technical support for LC-MS/MS analysis presented here.

Conflicts of Interest: We declare no current or potential conflict of interest related to this article.

References

1. Who No Time to Wait: Securing the Future from Drug-Resistant Infections. Available online: <https://www.who.int/antimicrobial-resistance/interagency-coordination-group/final-report/en/> (accessed on 31 December 2020).
2. O'Neill, J. *Tackling Drug-Resistant Infections Globally: Final Report and Recommendations*; The Government of the United Kingdom: London, UK, 2016.
3. Ali Mirza, S.; Afzaal, M.; Begum, S.; Arooj, T.; Almas, M.; Ahmed, S.; Younus, M. Chapter 11-Uptake Mechanism of Antibiotics in Plants. In *Antibiotics and Antimicrobial Resistance Genes in the Environment*; Hashmi, M.Z., Ed.; Elsevier: Amsterdam, The Netherlands, 2020; Volume 1, pp. 183–188. ISBN 9780128188828.
4. Michelin, D.C.; Moreschi, P.E.; Lima, A.C.; Nascimento, G.G.F.; Paganelli, M.O.; Chaud, M.V. Avaliação da atividade antimicrobiana de extratos vegetais. *Rev. Bras. Farmacogn.* **2005**, *15*, 316–320. [[CrossRef](#)]
5. Guarniz, W.A.S.; Canuto, K.M.; Ribeiro, P.R.V.; Dodou, H.V.; Magalhaes, K.N.; Sá, K.; do Nascimento, P.G.G.; Silva, K.L.; Sales, G.W.P.; Monteiro, M.P.; et al. *Momordica Charantia* L. Variety from Northeastern Brazil: Analysis of Antimicrobial Activity and Phytochemical Components. *Pharmacogn. J.* **2019**, *11*, 1312–1324. [[CrossRef](#)]
6. Lorenzi, H. *Plantas Daninhas Do Brasil: Terrestres, Aquáticas, Parasitas e Tóxicas*. 3ª edição. *Inst. Plant. Bras.* **2000**, *309*, 640.
7. Jia, S.; Shen, M.; Zhang, F.; Xie, J. Recent Advances in *Momordica Charantia*: Functional Components and Biological Activities. *Int. J. Mol. Sci.* **2017**, *18*, 2555. [[CrossRef](#)]
8. Bortolotti, M.; Mercatelli, D.; Polito, L. *Momordica Charantia*, a Nutraceutical Approach for Inflammatory Related Diseases. *Front. Pharmacol.* **2019**, *10*, 486. [[CrossRef](#)]
9. Gürdal, B.; Kültür, Ş. An Ethnobotanical Study of Medicinal Plants in Marmaris (Muğla, Turkey). *J. Ethnopharmacol.* **2013**, *146*, 113–126. [[CrossRef](#)] [[PubMed](#)]
10. Polito, L.; Bortolotti, M.; Maiello, S.; Battelli, M.; Bolognesi, A. Plants Producing Ribosome-Inactivating Proteins in Traditional Medicine. *Molecules* **2016**, *21*, 1560. [[CrossRef](#)]

11. Chen, J.; Tian, R.; Qiu, M.; Lu, L.; Zheng, Y.; Zhang, Z. Trinorcucurbitane and Cucurbitane Triterpenoids from the Roots of *Momordica Charantia*. *Phytochemistry* **2008**, *69*, 1043–1048. [[CrossRef](#)]
12. Polito, L.; Djemil, A.; Bortolotti, M. Plant Toxin-Based Immunotoxins for Cancer Therapy: A Short Overview. *Biomedicines* **2016**, *4*, 12. [[CrossRef](#)]
13. Grover, J.K.; Yadav, S.P. Pharmacological Actions and Potential Uses of *Momordica Charantia*: A Review. *J. Ethnopharmacol.* **2004**, *93*, 123–132. [[CrossRef](#)]
14. Raman, A.; Lau, C. Anti-Diabetic Properties and Phytochemistry of *Momordica Charantia* L. (Cucurbitaceae). *Phytomedicine* **1996**, *2*, 349–362. [[CrossRef](#)]
15. Bailey, C.J.; Day, C.; Leatherdale, B.A. Traditional Treatments for Diabetes from Asia and the West Indies. *Pract. Diabetes Int.* **1986**, *3*, 190–192. [[CrossRef](#)]
16. Dans, A.M.L.; Villarruz, M.V.C.; Jimeno, C.A.; Javelosa, M.A.U.; Chua, J.; Bautista, R.; Velez, G.G.B. The Effect of *Momordica Charantia* Capsule Preparation on Glycemic Control in Type 2 Diabetes Mellitus Needs Further Studies. *J. Clin. Epidemiol.* **2007**, *60*, 554–559. [[CrossRef](#)] [[PubMed](#)]
17. Hussein, R.A.; El-Anssary, A.A. Plants Secondary Metabolites: The Key Drivers of the Pharmacological Actions of Medicinal Plants. In *Herbal Medicine*; IntechOpen: London, UK, 2019.
18. Lei, Z.; Huhman, D.V.; Sumner, L.W. Mass Spectrometry Strategies in Metabolomics. *J. Biol. Chem.* **2011**, *286*, 25435–25442. [[CrossRef](#)] [[PubMed](#)]
19. Kim, H.W.; Choi, S.Y.; Jang, H.S.; Ryu, B.; Sung, S.H.; Yang, H. Exploring Novel Secondary Metabolites from Natural Products Using Pre-Processed Mass Spectral Data. *Sci. Rep.* **2019**, *9*, 17430. [[CrossRef](#)]
20. Graça, G.; Cai, Y.; Lau, C.-H.E.; Vorkas, P.A.; Lewis, M.R.; Want, E.J.; Herrington, D.; Ebbels, T.M.D. Automated Annotation of Untargeted All-Ion Fragmentation LC–MS Metabolomics Data with MetaboAnnotatoR. *Anal. Chem.* **2022**, *94*, 3446–3455. [[CrossRef](#)]
21. Wang, M.; Carver, J.J.; Phelan, V.V.; Sanchez, L.M.; Garg, N.; Peng, Y.; Nguyen, D.D.; Watrous, J.; Kapon, C.A.; Luzzatto-Knaan, T.; et al. Sharing and Community Curation of Mass Spectrometry Data with Global Natural Products Social Molecular Networking. *Nat. Biotechnol.* **2016**, *34*, 828–837. [[CrossRef](#)]
22. Gomes, P.W.P.; Barretto, H.; Reis, J.D.E.; Muribeca, A.; Veloso, A.; Albuquerque, C.; Teixeira, A.; Braamcamp, W.; Pamplona, S.; Silva, C.; et al. Chemical Composition of Leaves, Stem, and Roots of *Peperomia Pellucida* (L.) Kunth. *Molecules* **2022**, *27*, 1847. [[CrossRef](#)]
23. Gomes, P.; Quirós-Guerrero, L.; Muribeca, A.; Reis, J.; Pamplona, S.; Lima, A.H.; Trindade, M.; Silva, C.; Souza, J.N.S.; Boutin, J.; et al. Constituents of *Chamaecrista Diphylla* (L.) Greene Leaves with Potent Antioxidant Capacity: A Feature-Based Molecular Network Dereplication Approach. *Pharmaceutics* **2021**, *13*, 681. [[CrossRef](#)] [[PubMed](#)]
24. Gomes, P.W.P.; Pamplona, T.C.D.L.; Navegantes-Lima, K.C.; Quadros, L.B.G.; Oliveira, A.L.B.; Santos, S.M.; e Silva, C.Y.Y.; Silva, M.J.C.; Souza, J.N.S.; Quirós-Guerrero, L.M.; et al. Chemical Composition and Antibacterial Action of *Stryphnodendron Pulcherrimum* Bark Extract, “Barbatimão” Species: Evaluation of Its Use as a Topical Agent. *Arab. J. Chem.* **2021**, *14*, 103183. [[CrossRef](#)]
25. Gomes, P.; Quirós-Guerrero, L.; Silva, C.; Pamplona, S.; Boutin, J.A.; Eberlin, M.; Wolfender, J.-L.; Silva, M. Feature-Based Molecular Network-Guided Dereplication of Natural Bioactive Products from Leaves of *Stryphnodendron Pulcherrimum* (Willd.) Hochr. *Metabolites* **2021**, *11*, 281. [[CrossRef](#)] [[PubMed](#)]
26. Santiago, J.C.C.; Albuquerque, C.A.B.; Muribeca, A.d.J.B.; Sá, P.R.C.; Pamplona, S.d.G.S.R.; Silva, C.Y.Y.e.; Ribera, P.C.; Fontes-Júnior, E.d.A.; da Silva, M.N. *Margaritaria Nobilis* L.f. (Phyllanthaceae): Ethnopharmacology and Application of Computational Tools in the Annotation of Bioactive Molecules. *Metabolites* **2022**, *12*, 681. [[CrossRef](#)] [[PubMed](#)]
27. Holman, J.D.; Tabb, D.L.; Mallick, P. Employing ProteoWizard to Convert Raw Mass Spectrometry Data. *Curr. Protoc. Bioinform.* **2014**, *46*, 1–9. [[CrossRef](#)] [[PubMed](#)]
28. Pluskal, T.; Castillo, S.; Villar-Briones, A.; Oresic, M. MZmine 2: Modular Framework for Processing, Visualizing, and Analyzing Mass Spectrometry-Based Molecular Profile Data. *BMC Bioinform.* **2010**, *11*, 395. [[CrossRef](#)] [[PubMed](#)]
29. Shannon, P.; Markiel, A.; Ozier, O.; Baliga, N.S.; Wang, J.T.; Ramage, D.; Amin, N.; Schwikowski, B.; Ideker, T. Cytoscape: A Software Environment for Integrated Models of Biomolecular Interaction Networks. *Genome Res.* **2003**, *13*, 2498–2504. [[CrossRef](#)]
30. Lee, S.; van Santen, J.A.; Farzaneh, N.; Liu, D.Y.; Pye, C.R.; Baumeister, T.U.H.; Wong, W.R.; Lington, R.G. NP Analyst: An Open Online Platform for Compound Activity Mapping. *ACS Cent. Sci.* **2022**, *8*, 223–234. [[CrossRef](#)] [[PubMed](#)]
31. CLSI M100-S11. Performance Standards for Antimicrobial Susceptibility Testing. *Clin. Microbiol. Newsl.* **2001**, *23*, 49. [[CrossRef](#)]
32. Tortora, G.J.; Funke, B.R.; Case, C.L.; Weber, D.; Bair, W. *Microbiology*, 13th ed.; Pearson: London, UK, 2018; ISBN 9780134605180.
33. Osonga, F.J.; Akgul, A.; Miller, R.M.; Eshun, G.B.; Yazgan, I.; Akgul, A.; Sadik, O.A. Antimicrobial Activity of a New Class of Phosphorylated and Modified Flavonoids. *ACS Omega* **2019**, *4*, 12865–12871. [[CrossRef](#)]
34. Kuete, V. Potential of Cameroonian Plants and Derived Products against Microbial Infections: A Review. *Planta Med.* **2010**, *76*, 1479–1491. [[CrossRef](#)]
35. Jabeen, U.; Khanum, A. Isolation and Characterization of Potential Food Preservative Peptide from *Momordica Charantia* L. *Arab. J. Chem.* **2017**, *10*, S3982–S3989. [[CrossRef](#)]
36. Sumner, L.W.; Amberg, A.; Barrett, D.; Beale, M.H.; Beger, R.; Daykin, C.A.; Fan, T.W.-M.; Fiehn, O.; Goodacre, R.; Griffin, J.L.; et al. Proposed Minimum Reporting Standards for Chemical Analysis. *Metabolomics* **2007**, *3*, 211–221. [[CrossRef](#)] [[PubMed](#)]

37. Amaral, J.G.; Bauermeister, A.; Pilon, A.C.; Gouvea, D.R.; Sakamoto, H.T.; Gobbo-Neto, L.; Lopes, J.L.C.; Lopes, N.P. Fragmentation Pathway and Structural Characterization of New Glycosylated Phenolic Derivatives from *Eremanthus Glomerulatus* Less (Asteraceae) by Electrospray Ionization Tandem Mass Spectrometry. *J. Mass Spectrom.* **2017**, *52*, 783–787. [[CrossRef](#)] [[PubMed](#)]
38. Bittremieux, W.; Avalon, N.E.; Thomas, S.P.; Kakhkhorov, S.A.; Aksenov, A.A.; Gomes, P.W.P.; Aceves, C.M.; Rodriguez, A.M.C.; Gauglitz, J.M.; Gerwick, W.H.; et al. Open Access Repository-Scale Propagated Nearest Neighbor Suspect Spectral Library for Untargeted Metabolomics. *bioRxiv* **2022**. [[CrossRef](#)]
39. Li, A.; Hou, X.; Wei, Y. Fast Screening of Flavonoids from Switchgrass and *Mikania Micrantha* by Liquid Chromatography Hybrid-Ion Trap Time-of-Flight Mass Spectrometry. *Anal. Methods* **2018**, *10*, 109–122. [[CrossRef](#)]
40. Colombo, R.; Yariwake, J.H.; McCullagh, M. Study of C- and O-Glycosylflavones in Sugarcane Extracts Using Liquid Chromatography: Exact Mass Measurement Mass Spectrometry. *J. Braz. Chem. Soc.* **2008**, *19*, 483–490. [[CrossRef](#)]
41. March, R.; Brodbelt, J. Analysis of Flavonoids: Tandem Mass Spectrometry, Computational Methods, and NMR. *J. Mass Spectrom.* **2008**, *43*, 1581–1617. [[CrossRef](#)]
42. Kumar, S.; Singh, A.; Kumar, B. Identification and Characterization of Phenolics and Terpenoids from Ethanolic Extracts of *Phyllanthus* Species by HPLC-ESI-QTOF-MS/MS. *J. Pharm. Anal.* **2017**, *7*, 214–222. [[CrossRef](#)]
43. Du, L.-Y.; Zhao, M.; Xu, J.; Qian, D.-W.; Jiang, S.; Shang, E.-X.; Guo, J.-M.; Duan, J.-A. Analysis of the Metabolites of Isorhamnetin 3-O-Glucoside Produced by Human Intestinal Flora in Vitro by Applying Ultraperformance Liquid Chromatography/Quadrupole Time-of-Flight Mass Spectrometry. *J. Agric. Food Chem.* **2014**, *62*, 2489–2495. [[CrossRef](#)]
44. Chen, Y.; Yu, H.; Wu, H.; Pan, Y.; Wang, K.; Jin, Y.; Zhang, C. Characterization and Quantification by LC-MS/MS of the Chemical Components of the Heating Products of the Flavonoids Extract in Pollen *Typhae* for Transformation Rule Exploration. *Molecules* **2015**, *20*, 18352–18366. [[CrossRef](#)]
45. Nagy, R.; Grob, H.; Weder, B.; Green, P.; Klein, M.; Frelet-Barrand, A.; Schjoerring, J.K.; Brearley, C.; Martinoia, E. The Arabidopsis ATP-Binding Cassette Protein AtMRP5/AtABCC5 Is a High Affinity Inositol Hexakisphosphate Transporter Involved in Guard Cell Signaling and Phytate Storage. *J. Biol. Chem.* **2009**, *284*, 33614–33622. [[CrossRef](#)]
46. Desai, M.; Rangarajan, P.; Donahue, J.L.; Williams, S.P.; Land, E.S.; Mandal, M.K.; Phillippy, B.Q.; Perera, I.Y.; Raboy, V.; Gillasp, G.E. Two Inositol Hexakisphosphate Kinases Drive Inositol Pyrophosphate Synthesis in Plants. *Plant J.* **2014**, *80*, 642–653. [[CrossRef](#)] [[PubMed](#)]
47. Raboy, V. Seed Total Phosphate and Phytic Acid. In *Molecular Genetic Approaches to Maize Improvement*; Kriz, A.L., Larkins, B.A., Eds.; Springer: Berlin/Heidelberg, Germany, 2009; pp. 41–53. ISBN 9783540689225.
48. Freed, C.; Adepoju, O.; Gillasp, G. Can Inositol Pyrophosphates Inform Strategies for Developing Low Phytate Crops? *Plants* **2020**, *9*, 115. [[CrossRef](#)]
49. Chan, L.Y.; Wang, C.K.L.; Major, J.M.; Greenwood, K.P.; Lewis, R.J.; Craik, D.J.; Daly, N.L. Isolation and Characterization of Peptides from *Momordica Cochinchinensis* Seeds. *J. Nat. Prod.* **2009**, *72*, 1453–1458. [[CrossRef](#)] [[PubMed](#)]
50. Li, Z.; Tu, Z.; Wang, H.; Zhang, L. Ultrasound-Assisted Extraction Optimization of α -Glucosidase Inhibitors from *Ceratophyllum Demersum* L. and Identification of Phytochemical Profiling by HPLC-QTOF-MS/MS. *Molecules* **2020**, *25*, 4507. [[CrossRef](#)]
51. Kai, H.; Baba, M.; Okuyama, T. Two New Megastigmanes from the Leaves of *Cucumis Sativus*. *Chem. Pharm. Bull.* **2007**, *55*, 133–136. [[CrossRef](#)] [[PubMed](#)]
52. Ma, J.; Krynitsky, A.J.; Grundel, E.; Rader, J.I. Quantitative Determination of Cucurbitane-Type Triterpenes and Triterpene Glycosides in Dietary Supplements Containing Bitter Melon (*Momordica Charantia*) by HPLC-MS/MS. *J. AOAC Int.* **2012**, *95*, 1597–1608. [[CrossRef](#)] [[PubMed](#)]
53. Ferreira, M.-J.U.; Duarte, N.; Reis, M.; Madureira, A.M.; Molnár, J. Euphorbia and *Momordica* Metabolites for Overcoming Multidrug Resistance. *Phytochem. Rev.* **2014**, *13*, 915–935. [[CrossRef](#)]
54. Ramalhete, C.; Mansoor, T.A.; Mulhovo, S.; Molnár, J.; Ferreira, M.-J.U. Cucurbitane-Type Triterpenoids from the African Plant *Momordica Balsamina*. *J. Nat. Prod.* **2009**, *72*, 2009–2013. [[CrossRef](#)]
55. Dixon, R.A.; Howles, P.A.; Lamb, C.; He, X.Z.; Reddy, J.T. Prospects for the Metabolic Engineering of Bioactive Flavonoids and Related Phenylpropanoid Compounds. *Adv. Exp. Med. Biol.* **1998**, *439*, 55–66. [[CrossRef](#)]
56. Alcaráz, L.E.; Blanco, S.E.; Puig, O.N.; Tomás, F.; Ferretti, F.H. Antibacterial Activity of Flavonoids Against Methicillin-Resistant *Staphylococcus Aureus* Strains. *J. Theor. Biol.* **2000**, *205*, 231–240. [[CrossRef](#)]
57. Mirzoeva, O.K.; Grishanin, R.N.; Calder, P.C. Antimicrobial Action of Propolis and Some of Its Components: The Effects on Growth, Membrane Potential and Motility of Bacteria. *Microbiol. Res.* **1997**, *152*, 239–246. [[CrossRef](#)]
58. Kołpa, M.; Wałaszek, M.; Gniadek, A.; Wolak, Z.; Dobrosz, W. Incidence, Microbiological Profile and Risk Factors of Healthcare-Associated Infections in Intensive Care Units: A 10 Year Observation in a Provincial Hospital in Southern Poland. *Int. J. Environ. Res. Public Health* **2018**, *15*, 112. [[CrossRef](#)] [[PubMed](#)]
59. Hodek, P. Flavonoids. In *Metabolism of Drugs and Other Xenobiotics*; Wiley-VCH Verlag GmbH & Co. KGaA: Weinheim, Germany, 2012; pp. 543–582. ISBN 9783527630905.

60. Lin, R.-D.; Chin, Y.-P.; Lee, M.-H. Antimicrobial Activity of Antibiotics in Combination with Natural Flavonoids against Clinical Extended-Spectrum Beta-Lactamase (ESBL)-Producing *Klebsiella Pneumoniae*. *Phytother. Res.* **2005**, *19*, 612–617. [[CrossRef](#)] [[PubMed](#)]
61. Wang, E.; Li, Y.; Maguy, B.L.; Lou, Z.; Wang, H.; Zhao, W.; Chen, X. Separation and Enrichment of Phenolics Improved the Antibiofilm and Antibacterial Activity of the Fractions from *Citrus Medica* L. *Var. Sarcodactylis in Vitro and in Tofu*. *Food Chem.* **2019**, *294*, 533–538. [[CrossRef](#)] [[PubMed](#)]